Graphical Abstract

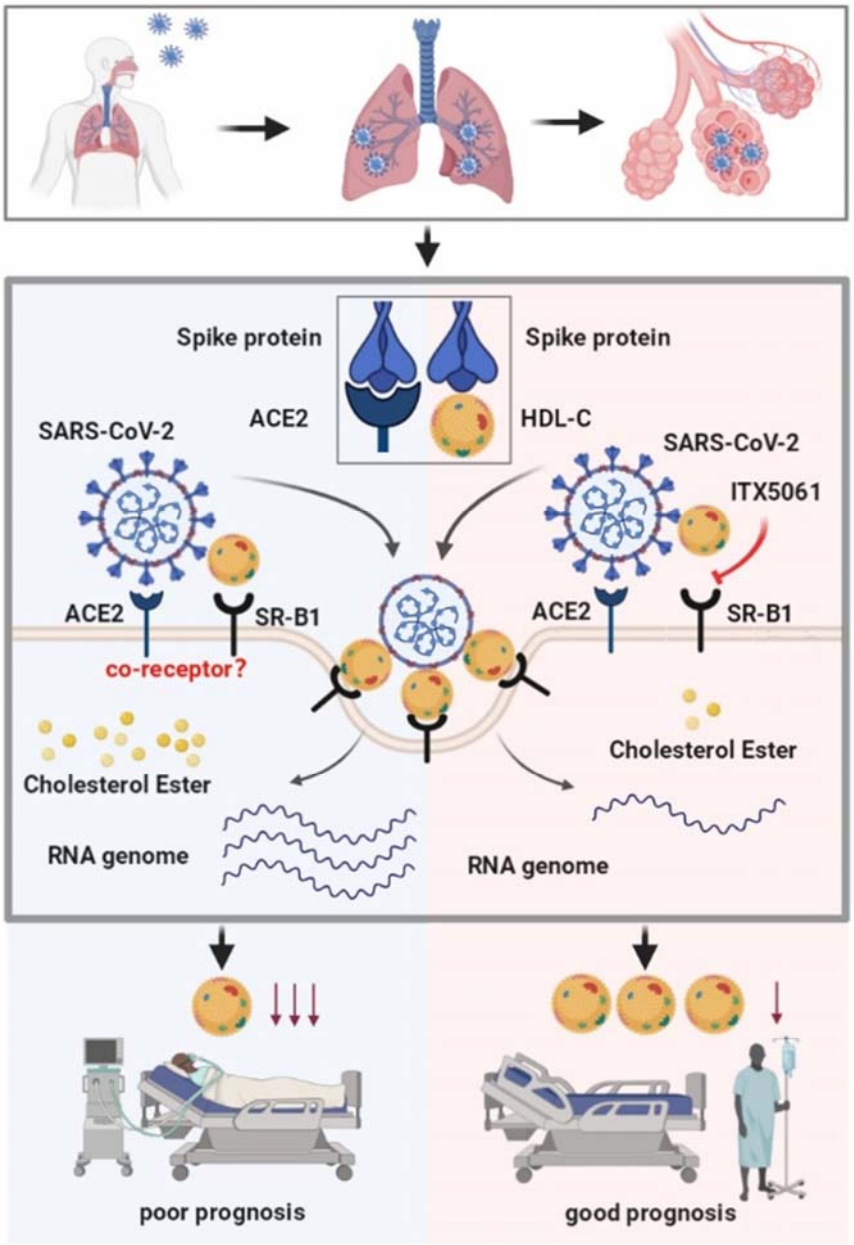

Cholesterol Metabolism—Impacts on SARS-CoV-2 Infection Prognosis, Entry, and Antiviral Therapies

Congwen Wei[1,8], Luming Wan[1,8], Yanhong Zhang[1,8], Chen Fan[2,8], Qiulin Yan[1], Xiaoli Yang[3], Jing Gong[1], Huan Yang[1], Huilong Li[1], Jun Zhang[1], Zhe Zhang[1], Rong Wang[1], Xiaolin Wang[1], Jin Sun[1], Yulong Zong[4], Feng Yin[5], Rui Zhang[6], Qi Gao[7]*, Yuan Cao[2]* and Hui Zhong[1]*

1 Beijing Institute of Biotechnology, Beijing, 100850, China.

2 Department of Laboratory Medicine, the 960th Hospital of PLA, Jinan, 250031, China.

3 Department of Clinical Laboratory, the Third Medical Centre, Chinese PLA General Hospital, 100850, China.

4 Department of Laboratory Medicine, Taian City Central Hospital, Taian, 271000, China.

5 Department of Laboratory Medicine, Taian City Central Hospital Branch, Taian, 271000, China.

6 Cancer Hospital of China Medical University, Liaoning Cancer Hospital and Institute, Shenyang, 110042, China

7 Hotgen Biotech Co., Ltd. Beijing, 102600, China

8 These authors contributed equally to this work

*Correspondence : gaoqi@hotgen.com(Q.G.); labs.net@gmail.com(Y.C.); towall@yahoo.com(H.Z.).

Running title: SARS-CoV-2 modulates the cholesterol metabolism

Abstract

The recently emerged pathogenic SARS-coronavirus 2 (SARS-CoV-2) has spread rapidly, leading to a global pandemic. In this study, we show that SARS-CoV-2 infection was associated with clinically significant lower level of HDL cholesterol (HDL-C), which can be used as indicators of disease severity and poor prognosis. Importantly, we found the spike protein of SARS-CoV-2 (SARS-2-S) bound to HDL. Antagonists of HDL receptor-Scavenger receptor class B type I (SR-B1), strongly inhibited SARS-CoV-2 infection. Notably, the lipids transfer function of SR-B1 was indispensable for this inhibition, offering explanations for the reduced serum HDL level observed in COVID-19 patients. Basing on findings here, we speculate that SR-B1-mediated pulmonary HDL-vitamin E uptake could participate in mediating SARS-CoV-2 infection of lung cells, and the unique expression profile of SR-B1 may also affect SARS-CoV-2 cell and tissue tropism. These findings might help to provide further insights into viral transmission, pathological characteristics and reveal therapeutic targets.

Introduction

Since the outbreak of COVID-19 caused by severe acute respiratory syndrome coronavirus 2 (SARS-CoV-2), more than a million SARS-CoV-2 cases have been reported in over 200 countries [1]. SARS-CoV-2 virions are approximately 90 to 120 nm in diameter and contain four structural proteins including the spike (S) protein, nucleocapsid (N) protein, envelope (E) protein, and membrane (M) protein [2]. S glycoprotein forms homotrimers protruding from the viral surface and comprises S1 and S2 functional subunits responsible for binding and fusion (Tortorici and Veesler, 2019).

Enveloped viruses enter cells by two primary pathways, typically via direct fusion with the plasma membrane at the cell surface or receptor mediated endocytosis. Most viruses use only one of these pathways to enter cells, while some viruses use multiple mechanisms to gain entry into host cells [3,4]. SARS-CoV enters cells through the endocytic pathway after direct fusion with the plasma membrane. SARS-CoV-2 is closely related to SARS-CoV, with ~76% amino acid identity. Both viruses use angiotensin-converting enzyme 2 (ACE2) as the entry receptor and employ the cellular serine protease TMPRSS2 for S protein priming [5,6]. In addition to ACE2, CD147 facilitates SARS-CoV-2 entry into host cells [7]; however, other coreceptors or cellular molecules may be required for SARS-CoV-2 entry.

Cholesterol homeostasis is vital for proper cellular and systemic functions. Excess cholesterol is either stored as cytosolic lipid droplets or released as plasma lipoproteins, including chylomicrons, VLDL, LDL and HDL cholesterol. Circulating

lipoproteins can be taken up by binding to their receptors without parallel apolipoprotein uptake, a process known as the selective cholesterol uptake pathway. Scavenger receptor B type 1 (SR-B1) is a cell surface HDL receptor that mediates the selective uptake of HDL-CE (cholesteryl esters) and other lipid components of receptor bound HDL particles, including free cholesterol (FC), triglycerides (TG), phospholipids (PL),α-tocopherol and vitamin E . This cholesterol delivery system is well operated in isolated hepatocytes, fibroblasts, adipocytes, macrophages, adrenal, ovarian and testicular Leydig cells. Interestingly, alveolar type II cells also express SR-B1, which is responsible for vitamin E uptake preferentially from HDL. SR-B1 emerges as critical receptors affecting dengue and HCV entry [8], however, the possible role of SR-B1 in SARS-CoV-2 infection has never been revealed.

In this study, we performed a retrospective study involving 861 COVID-19 patients classified as mild, moderate, severe or critical. The serum concentrations of TC and HDL-C can be used as indicators of disease severity and prognosis in COVID-19 patients. Mechanistically, SARS-2-S bound to HDL and SARS-CoV-2 manipulated SR-B1-mediated HDL uptake pathway to facilitate its entry. SR-B1 antagonists ITX 5061 and BLT1 inhibited SARS-CoV-2 pseudovirus infection. The transport function of SR-B1 in alveolar type II cells indicates its potential important role in mediating SARS-CoV-2 infection of lung cells.

Methods

Materials Availability and Data and Code Availability

All unique/stable reagents generated in this study are available from the Lead Contact with a completed Materials Transfer Agreement. The number of replicates carried out for each experiment is described in the figure/table legends. The Graphical Abstract was created with BioRender.com under a paid subscription.

Materials

His-tagged SARS-CoV-2 Spike (SARS-CoV-2-S), S1, and S2 recombinant proteins were purchased from Sino Biological Inc. (40589-V08B1, 40591-V08H and 40591-V08B, respectively). ITX 5061 and BLT1 were purchased from MedChemExpress Incorporation (HY-19900) and Sigma-Aldrich Incorporation (SML0059), respectively. HDL-C was purchased from Sigma-Aldrich Incorporation (L8039).

Data sources

This study was approved by the Ethics Committee of the TaiKang Tongji hospital ([2020] TKTJLL-003). As we collected the data from electronic medical files without contacting with the patients directly or analyzing the serum, written informed consent was waived. The basic informations and serum biochemical test results were collected from 861 COVID-19 patients in TaiKang Tongji Hospital (Wuhan, Hubei province, People's Republic of China) from February 16 to March 20, 2020. The median age was 60 years (range 16-96 years). Serum lipid profiles from 1108 age- and sex-matched individuals from the Third Medical Center of the Chinese PLA General Hospital were used as reference values. The median age was 61 years (range

31-96 years). The clinical and biochemical characteristics of these individuals were given in Table 1. The age and sex distributions did not differ between these two groups.

Clinical manifestations were used to classify the disease status into four categories: mild, moderate, severe and critical. Mild clinical disease was characterized by mild symptoms with no pulmonary inflammation visible upon imaging. Disease was classified as moderate in the overwhelming majority of patients, who showed symptoms of respiratory infection, such as fever, cough, and sputum production, with pulmonary inflammation visible upon imaging. Disease was classified as severe when symptoms of dyspnea appeared, as assessed by the following symptoms: shortness of breath, respiration rate (RR) ≥ 30 bpm, resting blood oxygen saturation ≤ 93%, partial pressure of arterial oxygen/fraction of inspired oxygen ratio (PaO2/FiO2) ≤ 300 mmHg, or pulmonary inflammation that progressed significantly (> 50%) within 24 to 48 h. Critical disease was classified as the presence of respiratory failure, shock, or organ failure that required intensive care. Infection was confirmed in all patients by viral detection using quantitative RT-PCR, which simultaneously ruled out infection by other respiratory viruses, such as influenza virus A, influenza virus B, Coxsackie virus, respiratory syncytial virus, parainfluenza virus and enterovirus. All cases were diagnosed and classified according to the New Coronavirus Pneumonia Diagnosis Program (6th edition) published by the National Health Commission of China. Among the patients, 216 cases were classified as mild, 363 as moderate, 217 as severe and 65 cases as critical (Table 1).

Cell lines

293T (human kidney), Huh7 (human hepatoma), and Vero (African green monkey kidney) cells were incubated in Dulbecco's modified Eagle's medium (Gibco). All cell lines were incubated at 37°C and 5% CO_2 in a humidified atmosphere and had previously been tested for mycoplasma contamination. Lipofectamine 2000 (Invitrogen) reagent was used for transfection following the manufacturer's protocol.

Plasmid

Codon-optimized cDNA encoding SARS-CoV-2-S (QHU36824.1) with a C-terminal 19 amino acid deletion was synthesized and cloned into the eukaryotic expression vector pcDNA3.1 (Invitrogen).

Pseudotyped virus infection assays

293T cells were cotransfected with pNL4-3.Luc.R-E- (the luciferase reporter-expressing HIV-1 backbone) and pcDNA3.1-SARS-CoV-2-S (encoding for SARS-CoV-2 S protein) using Lipofectamine 2000. Pseudotyped particles were efficiently released in the supernatant. The supernatant was harvested at 72 h post-transfection, centrifuged at 2000× g for 5 min, and frozen to −80 °C.

To detect the inhibitory activity of ITX 5061 or BLT-1, Huh-7 cells were plated at a density of 10^4 cells per well in a 96-well plate. Huh-7 cells were incubated with ITX 5061, BLT-1 or DMSO control for 5 h prior to infection. Medium was changed after 12 h and incubation continued for 48 h. Luciferase activity was analyzed by the Luciferase Assay System.

Microscale thermophoresis (MST)

MST assay was conducted as previously described [9]. In brief, protein samples were labeled and mixed with cholesterol or HDL at the indicated concentrations at room temperature. Fluorescence was determined in a thermal gradient generated by a Monolith NT.115 system (NanoTemper Technologies), and the data were analyzed with MOAffinityAnalysis v2.1.23333.

Statistical methods

In this study, GraphPad 6.0 software was used for statistical calculations and data plotting. All statistical analyses were performed using SPSS version 20 (SPSS, Chicago, IL, USA). Differences between two independent samples were evaluated by a t-test or Mann-Whitney U test. Differences between multiple samples were analyzed by one-way ANOVA followed by Bonferroni's post hoc analysis. Analysis of variance or the Kruskal-Wallis rank sum test was used for comparisons among multiple groups. The chi-square test was performed to compare count data. Significance values were set at: ns (not significant), $p > 0.05$; *, $P < 0.05$; **, $P < 0.01$; ***, $P < 0.001$.

Results

SARS-CoV-2 infection is associated with clinically significant lower levels of TC and HDL-C

Liver damage infected with SARS-CoV-2 prompted us to investigate whether infection with this virus could lead to alterations in lipid metabolism. The serum lipid levels of each subject showed that total TG levels were similar between the reference population and the COVID-19 patients (P =0.062; Table 1 and Figure 1A),

but the serum TC and HDL-C levels were significantly lower in COVID-19 patients than in the reference population (P <0.0001 and P <0.0001, respectively; Table 1 and Figure 1B-C). Thus, SARS-CoV-2 infection was associated with clinically significant lower levels of TC and HDL-C. Interestingly, COVID-19 patients had significantly higher serum LDL-C levels than age- and sex-matched adults from the reference population (P < 0.0001; Table 1 and Figure 1D).

Cholesterol levels are inversely associated with disease severity in COVID-19 patients

We next sought to determine whether serum lipid levels were correlated with disease conditions in COVID-19 patients. Although serum TG levels were significantly lower in patients with moderate disease than in those with mild disease (P< 0.0001; Table 2 and Figure 2A), they were similar in moderately, severely and critically ill patients (Table 2 and Figure 2A). However, the serum TC (Table 2 and Figure 2B), HDL-C (Table 2 and Figure 2C), and LDL-C (Table 2 and Figure 2D) concentrations were negatively correlated with disease severity and were particularly lower in critically ill patients than in patients with less severe disease. Specifically, the median HDL-C concentration in critically ill patients was 0.888 mmol/L (Table 2), which was below the normal range (1.03-1.89 mmol/L). Collectively, these results indicate that serum cholesterol levels may reflect the disease progression in patients infected with SARS-CoV-2.

TC and HDL-C levels have prognostic value for COVID-19 patients with severe disease

We then selected 100 patients with severe symptoms but a cured outcome (survivors) and 16 with severe symptoms that died (non-survivors) and compared their lipid levels at admission (pretherapy) and after therapy (posttherapy). Although both groups of patients showed similar TG levels before and after therapy (Figure 3A), the TC and HDL-C levels of survivors rose significantly after therapy but dropped significantly in non-survivors (Figure 3B-C). LDL-C levels remained unchanged in survivors but decreased significantly after therapy (Figure 3D). In addition, we randomly selected 11 survivors and 9 non-survivors and monitored the dynamic changes in the HDL-C level of each patient from admission to recovery or death. Although the disease course differed in each patient, the HDL-C level increased progressively in 8 out of 11 survivors (Figure 3E), whereas the HDL-C level in all non-survivors showed a progressive decreasing trend (Figure 3F). Taken together, these results suggest that TC and HDL-C levels are prognostic predictors in patients with severe disease caused by SARS-CoV-2 infection.

SR-B1 Antagonist Blocks SARS-CoV-2 Infection

Since SARS-CoV-2 infection led to a reduced HDL-C level, we thus speculated that SARS-CoV-2 might manipulate the selective cholesterol transport pathway mediated by SR-B1 for its entry, in a way similar to HCV. To this end, we initially employed ITX 5061, a clinically proven SR-B1 antagonist that can increase HDL levels, and assessed its effect on SARS-CoV-2 infection. HIV pseudotypes bearing SARS-2-S were used to study cell entry of SARS-CoV-2. Huh7 cells showed high susceptibility for SARS-CoV-2 pseudotypes (Figure 4A). Accordingly, ITX 5061 strongly inhibited the entry of

SARS-2-S pseudovirus into host cells (Figure 4B). To assess the cytotoxicity of ITX 5061, we evaluated its effect on cell survival. Treatment with the indicated dose of ITX 5061 did not affect cell survival (Figure 4C). Moreover, Block lipid transport-1 (BLT-1), a small chemical widely used to inhibit the transfer of lipids between HDL and cells mediated by SR-B1, also significantly blocked SARS-2-S-driven entry into Huh7 cells (Figure 4D) and exerted no unwanted cytotoxic effects (Figure 4E). Notably, cholesterol enhanced SARS-2-S pseudovirus entry when presented during infection (Figure 4F). Together, our results indicated that SARS-CoV-2 manipulates the SR-B1 pathway for its entry.

SARS-2-S binds to cholesterol and HDL

The observation that SARS-CoV-2 manipulates the SR-B1 pathway for its entry prompted us to investigate the possible interaction of SARS-2-S with lipoprotein or cholesterol. A search for cholesterol-regulated motifs in the primary sequence of SARS-2-S identified 6 putative cholesterol recognition amino acid consensus (CRAC) motifs adjacent to the inverted cholesterol recognition motif called CARC [10] (Figure 5A). To evaluate the ability of SARS-2-S to bind to cholesterol, we purchased purified soluble SARS-2-S protein. This protein was incubated with cholesterol in 0.5% Fos-choline at concentrations ranging from 0.1 to 1000 nM, and interactions were assessed using MST. SARS-2-S interacted with cholesterol with an EC50 of 187.6±120.5 nM (Figure 5B). To continue this investigation, we analyzed the interaction of SARS-2-S, S1 and S2 with HDL particles. Remarkably, although both the full length spike protein and its S1 subunit bound to HDL, S had over 5-fold higher

affinity than S1 (Figure 5C). Interestingly, the S2 subunit of the S protein, which mediates fusion, failed to bind HDL (Figure 5D). These data indicate that SARS-CoV-2 may manipulates cholesterol metabolism via the SARS-2-S-HDL interaction.

Discussion

The present study provides evidence that SARS-CoV-2 entry is a multistep process with multiple receptors. Because of the association of SARS-2-S with HDL, the HDL receptor SR-B1 may contribute to uptake and cellular penetration of SARS-CoV-2, leading to the reduced serum levels of HDL-C and TC. ITX5061, a small-molecule SR-B1 antagonist that is a promising inhibitor of HCV infection [11], strongly inhibits SARS-CoV-2 infection, supporting the notion that SARS-CoV-2/HDL/SR-B1 interactions might influence the infectivity of SARS-CoV-2. The linking of cholesterol metabolism with SARS-CoV-2 infection not only enhances our understanding of the virus–host interaction, but also expands antiviral therapeutic approaches to include drugs that target lipid metabolism.

Here, we specifically addressed the connection between the SARS-CoV-2 virus with host cholesterol metabolism. The levels of both TG and HDL-C were significantly lower in patients with severe disease than in patients with moderate or mild disease. After successful treatment, cholesterol metabolism was reestablished in patients with SARS-CoV-2 infection. Metabolomic analysis of SARS-CoV-2 infection also showed massive metabolic suppression. Interestingly, although decreasing levels of LDL-C were associated with disease progression, COVID-19 patients had significantly

higher levels of LDL-C than normal adults matched for age and sex. Our unpublished data confirmed this result in COVID-19 patients from another hospital in Hubei. More data are needed to reveal the mechanism underlying the association of increased LDL-C levels with COVID-19.

Our results support a role for SR-B1, a protein related to the HDL-C life cycle, as a direct (co-)receptor in cell entry of SARS-CoV-2. SARS-2-S contains multiple CRAC motifs and CARC motif. Although these motifs alone might have low predictive value for identifying cholesterol-binding sites, the MST assay results confirmed the ability of SARS-2-S and S1 to bind HDL. Considering the reduced HDL levels, we speculated that an HDL-virion interaction may serve to facilitate viral entry through the uptake of lipoprotein particles rather than just bring the virus in proximity to other entry cofactors. Indeed, BLT-4, a small compound inhibiting the SR-B1-mediated selective transfer of lipids without affecting HDL-SR-B1 binding [12], strongly inhibits SARS-2-S infectivity. Thus, the expression of SR-B1 in intestine, macrophages, endothelial cells, smooth muscle cells, keratinocytes, adipocytes, steroidogenic cells and liver may contribute to the pathogenesis of SARS-CoV-2 infection. In addition, alveolar type II cells are responsible for synthesis, storage, and secretion of pulmonary surfactant enriched with vitamin E [13]. We know that HDL are the major sources of vitamin E, and SR-B1 expression in alveolar type II mediates vitamin E uptake from HDL [14]. Therefore, the transport function of SR-B1 in HDL-vitamin E uptake might play important roles in SARS-CoV-2 infection of lung cells. Much work remains to improve our understanding of the mechanisms underlying coordinate interactions with

multiple (co-)receptors in the setting of SARS-CoV-2 infection.

Immune dysfunctions are a common feature in cases of SARS-CoV-2 infection and might be critical factors associated with disease severity [15]. Here, we speculated that the immune-mediated cytokine storm might result at least partially from decreased HDL-C levels. HDL-C relieves cells of excessive amounts of cholesterol and has strong anti-inflammatory properties. In addition, HDL-C inhibits TLR-induced production of proinflammatory cytokines by macrophages [16]. Moreover, Clinical studies haves shown that higher systemic levels of HDL and apoA-I are associated with less severe air flow obstruction [17]. The correlation of reduced HDL-C levels with disease severity and mortality associated with SARS-CoV-2 infection implies the physiologically important function of HDL-C. HDL-C-mediated cholesterol efflux and selective cholesterol transport become dysfunctional in chronic metabolic diseases such as obesity or atherosclerosis, consistent with the increased mortality observed in elderly patients and patients with obesity or diabetes [18,19]. In addition, approximately half of the patients with SARS-CoV-2 infection had chronic underlying diseases, mainly cardiovascular and cerebrovascular diseases and diabetes [20]. Therefore, intensive surveillance and early evaluation of the serum lipid levels in patients with preexisting conditions, especially in older patients with other comorbidities, might be needed.

In conclusion, this study provided key insights into the remarkable capacity of SARS-CoV-2 virus to hijack SR-B1 functions in favoring of its entry and defined potential prognostic and antiviral approaches to interfere with virus entry.

Acknowledgements

This study was supported in part by grants from the National Key Research and Development Program of China (2018YFA0900800) and the National Natural Science Foundation of China (31670761, 31872715 and 81773205). The funders had no role in the study design, data collection and analysis, decision to publish, or preparation of the manuscript.

Author Contributions

C.W.W., Q.G., Y.C. and H.Z. designed the experiments. L.M.W., Y.H.Z. and C. F. collected and analyzed the data. Q.L.Y., H.Y., X.L.W. and J.S. carried out pseudovirus assays. J.G., J.Z., Z.Z. and R.W. carried out MST assys. H.L.L., Y.L.Z., F.Y., X.L.Y. and R.Z carried out cell lines experiments. C.W.W., L.M.W. and H.Z. analyzed the data and prepared the manuscript.

Declaration of Interests

The authors have declared that no competing interests exist.

References

1. WHO. Coronavirus disease (COVID-19) Pandemic: World Health Organization; 2020.
2. Chen N, Zhou M, Dong X, et al. Epidemiological and clinical characteristics of 99 cases of 2019 novel coronavirus pneumonia in Wuhan, China: a descriptive study. *The Lancet*. 2020;395(10223):507-513.
3. Wang H, Yang P, Liu K, et al. SARS coronavirus entry into host cells through a novel clathrin- and caveolae-independent endocytic pathway. *Cell Res*. 2008;18(2):290-301.
4. Pelkmans L, Helenius A. Insider information: what viruses tell us about endocytosis. *Curr Opin Cell Biol*. 2003;15(4):414-422.
5. Hoffmann M, Kleine-Weber H, Schroeder S, et al. SARS-CoV-2 Cell Entry Depends on ACE2 and TMPRSS2 and Is Blocked by a Clinically Proven Protease Inhibitor. *Cell*. 2020.
6. Walls AC, Park YJ, Tortorici MA, Wall A, McGuire AT, Veesler D. Structure, Function, and Antigenicity of the SARS-CoV-2 Spike Glycoprotein. *Cell*. 2020;181(2):281-292 e286.
7. Wang K, Chen W, Zhou Y-S, et al. SARS-CoV-2 invades host cells via a novel route: CD147-spike protein. 2020.

8. Catanese MT, Ansuini H, Graziani R, et al. Role of scavenger receptor class B type I in hepatitis C virus entry: kinetics and molecular determinants. *J Virol*. 2010;84(1):34-43.

9. Widenmaier SB, Snyder NA, Nguyen TB, et al. NRF1 Is an ER Membrane Sensor that Is Central to Cholesterol Homeostasis. *Cell*. 2017;171(5):1094-1109 e1015.

10. Fantini J, Di Scala C, Baier CJ, Barrantes FJ. Molecular mechanisms of protein-cholesterol interactions in plasma membranes: Functional distinction between topological (tilted) and consensus (CARC/CRAC) domains. *Chem Phys Lipids*. 2016;199:52-60.

11. Masson D, Koseki M, Ishibashi M, et al. Increased HDL cholesterol and apoA-I in humans and mice treated with a novel SR-BI inhibitor. *Arterioscler Thromb Vasc Biol*. 2009;29(12):2054-2060.

12. Nieland TJ, Chroni A, Fitzgerald ML, et al. Cross-inhibition of SR-BI- and ABCA1-mediated cholesterol transport by the small molecules BLT-4 and glyburide. *J Lipid Res*. 2004;45(7):1256-1265.

13. Kolleck I, Sinha P, Rustow B. Vitamin E as an antioxidant of the lung: mechanisms of vitamin E delivery to alveolar type II cells. *Am J Respir Crit Care Med*. 2002;166(12 Pt 2):S62-66.

14. Kolleck I, Schlame M, Fechner H, Looman AC, Wissel H, Rustow B. HDL is the major source of vitamin E for type II pneumocytes. *Free Radic Biol Med*. 1999;27(7-8):882-890.

15. Zhang C, Shi L, Wang FS. Liver injury in COVID-19: management and challenges. *Lancet Gastroenterol Hepatol*. 2020.

16. De Nardo D, Labzin LI, Kono H, et al. High-density lipoprotein mediates anti-inflammatory reprogramming of macrophages via the transcriptional regulator ATF3. *Nat Immunol*. 2014;15(2):152-160.

17. Gordon EM, Figueroa DM, Barochia AV, Yao X, Levine SJ. High-density Lipoproteins and Apolipoprotein A-I: Potential New Players in the Prevention and Treatment of Lung Disease. *Front Pharmacol*. 2016;7:323.

18. Assmann G, Gotto AM, Jr. HDL cholesterol and protective factors in atherosclerosis. *Circulation*. 2004;109(23 Suppl 1):III8-14.

19. Rashid S, Genest J. Effect of obesity on high-density lipoprotein metabolism. *Obesity (Silver Spring)*. 2007;15(12):2875-2888.

20. Lai CC, Liu YH, Wang CY, et al. Asymptomatic carrier state, acute respiratory disease, and pneumonia due to severe acute respiratory syndrome coronavirus 2 (SARS-CoV-2): Facts and myths. *J Microbiol Immunol Infect*. 2020.

Figure Legends

Figure 1. SARS-CoV-2 infection is associated with clinically significant lower levels of TC and HDL-C

(A-B) TG (A) and TC (B) levels in COVID-19 patients and reference subjects. Differences between the two groups were evaluated using the Mann-Whitney U test: ns, $p > 0.05$;*, $P < 0.05$; **, $P < 0.01$; ***, $P < 0.001$.

(C-D) HDL-C (C) and LDL-C (D) levels in COVID-19 patients and reference subjects. Differences between the two groups were evaluated using the Mann-Whitney U test: ns, $p > 0.05$; *, $P < 0.05$; **, $P < 0.01$; ***, $P < 0.001$.

Figure 2. Cholesterol levels are inversely associated with disease severity in COVID-19 patients

(A-B) Plot of TG (A) and TC (B) levels in COVID-19 patients with four different levels of disease severity. Differences among groups were evaluated using the Mann-Whitney U test: ns, $p > 0.05$; *, $P < 0.05$; **, $P < 0.01$; ***, $P < 0.001$.

(C-D) Plot of HDL-C (C) and LDL-C (D) levels in COVID-19 patients with four different levels of disease severity. Differences among groups were evaluated using the Mann-Whitney U test: ns, $p > 0.05$; *, $P < 0.05$; **, $P < 0.01$; ***, $P < 0.001$.

Figure 3. TC and HDL-C levels have prognostic value for COVID-19 patients with severe disease

(A-D) Changes in serum TG (A), TC (B), HDL-C (C) and LDL-C (D) levels in survivors and non-survivors before therapy (pretherapy) and after therapy (posttherapy). Differences between groups were evaluated using the Mann-Whitney U test: ns, p >

0.05; *, P < 0.05; **, P < 0.01; ***, P < 0.001.

(E-F) Temporal changes in serum HDL-C levels in survivors (E) and non-survivors (F) starting from illness onset.

Figure 4. SR-B1 Antagonist Blocks SARS-CoV-2 Infection

(A) Huh7 cells were inoculated with pseudovirus particles bearing SARS-2-S. At 48 h postinoculation, pseudotyped virus entry was analyzed by determining luciferase activity in cell lysates. Signals obtained without pseudovirus were used for normalization. Student's t-test was used for statistical analysis: ns, p > 0.05; *, P < 0.05; **, P < 0.01; ***, P < 0.001.

(B,D) Huh7 cells were preincubated with the indicated concentrations of ITX 5061 (B) or BLT-1 (D) and subsequently inoculated with pseudovirus particles bearing SARS-2-S. At 48 h postinoculation, pseudotyped virus entry was analyzed by determining luciferase activity in cell lysates. Signals obtained without compounds were used for normalization. One-way ANOVA followed by Bonferroni's post hoc analysis was used for statistical analysis: ns, p > 0.05; *, P < 0.05; **, P < 0.01; ***, P < 0.001.

(C,E) Huh7 cell were preincubated with the indicated concentrations of ITX 5061 (C) or BLT-1 (E). At 48 h postinoculation, MTT was added to the cells, and the OD492 value was measured. Signals obtained without compounds were used for normalization. One-way ANOVA followed by Bonferroni's post hoc analysis was used for statistical analysis: ns, p > 0.05; *, P < 0.05; **, P < 0.01; ***, P < 0.001.

(F) Huh7 cell were preincubated with the indicated concentrations of cholesterol and

subsequently inoculated with pseudovirus particles bearing SARS-2-S. At 48 h postinoculation, pseudotyped virus entry was analyzed by determining luciferase activity in cell lysates. Signals obtained without cholesterol were used for normalization. One-way ANOVA followed by Bonferroni's post hoc analysis was used for statistical analysis: ns, $p > 0.05$; *, $P < 0.05$; **, $P < 0.01$; ***, $P < 0.001$.

Cell-based studies were performed at least three times independently with comparable results. Data are presented as the means ± SEMs.

Figure 5. SARS-2-S binds to cholesterol and HDL

(A) Schematic illustration of the cholesterol-binding motif in SARS-2-S. Crucial amino acid residues in the CARC motif are highlighted in red, crucial amino acid residues in the CRAC motif are highlighted in green, and shared amino acid residues are highlighted in purple. The green stick indicates the CARC motif, and the red stick indicates the CRAC motif.

(B) Effect of cholesterol on fluorescence decay of fluorescently labeled SARS-2-S as evaluated with MST. EC50 was determined by Hill slope.

(C-D) Effect of HDL on fluorescence decay of fluorescently labeled SARS-2-S, -S1 (C) and -S2 (D) as evaluated with MST. EC50 was determined by Hill slope.

Table 1. Clinical characteristics of COVID-19 patients and reference controls

Characteristics	SARS-CoV-2 patients (n=861)	Reference populations (n=1108)	P-value
Age (years)	61.42 ± 14.73	60.44 ± 14.29	0.2207
Sex (M/F)	386/475	481/627	0.5289
TC (mg/dL)	4.637 ±1.130	5.069 ±1.024	< 0.0001
TG (mg/dL)	1.473 ± 1.081	1.574 ± 1.068	0.0623
HDL-C (mg/dL)	1.196 ±0.3237	1.512 ±0.3216	< 0.0001
LDL-C (mg/dL)	3.125 ±0.8618	2.573 ±0.7177	< 0.0001

Table 2. Clinical features of COVID-19 patients

Characteristics	Mild patients (n=216)	Moderate patients (n=363)	severe patients (n=217)	Critical patients (n=65)
Age (years)	55.22±12.29	58.57±14.88	68.41±12.02	74.55±12.32
Sex (M/F)	89/127	148/215	116/101	33/32
TC (mg/dL)	5.073±1.088	4.674±0.9489	4.470±1.143	3.625±1.276
TG (mg/dL)	1.702±1.584	1.375±0.7788	1.363±0.7304	1.628±1.209
HDL-C (mg/dL)	1.311±0.3021	1.232±0.2955	1.115±0.3011	0.888±0.240
LDL-C (mg/dL)	3.364±0.8137	3.165±0.7887	3.038±0.8916	2.395±0.880

Figure 1

A

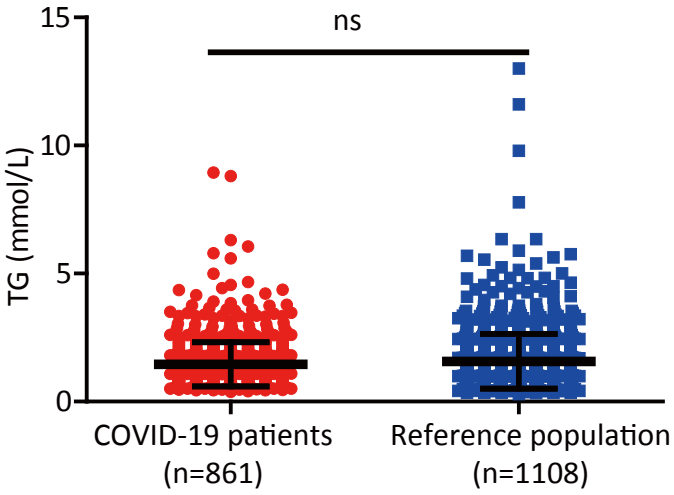

B

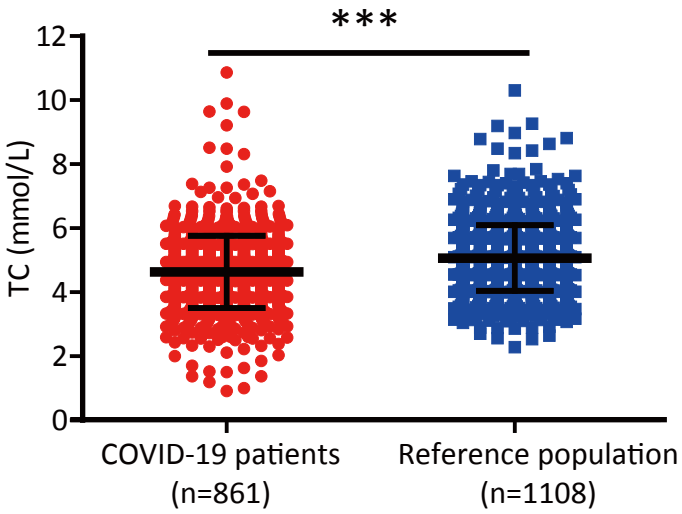

C

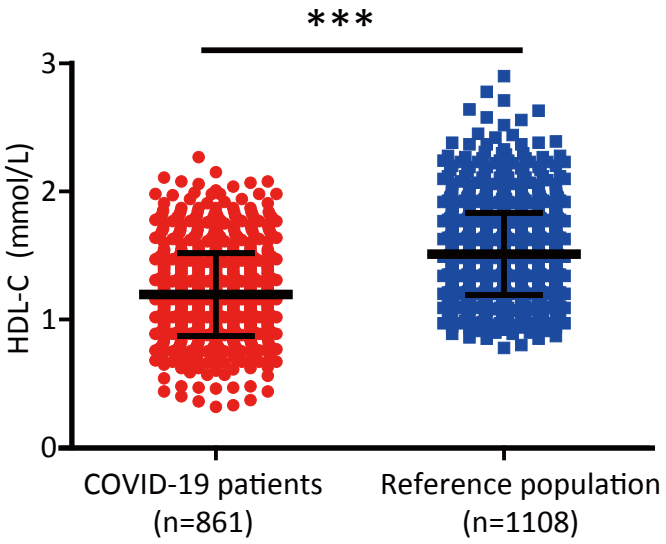

D

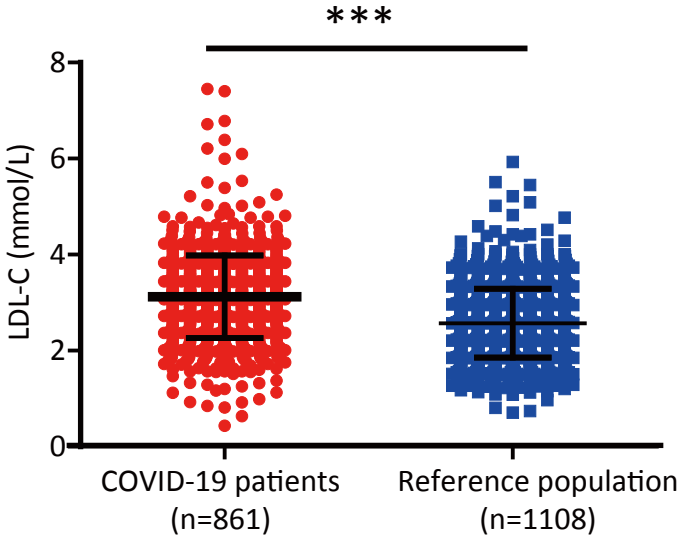

Figure 2

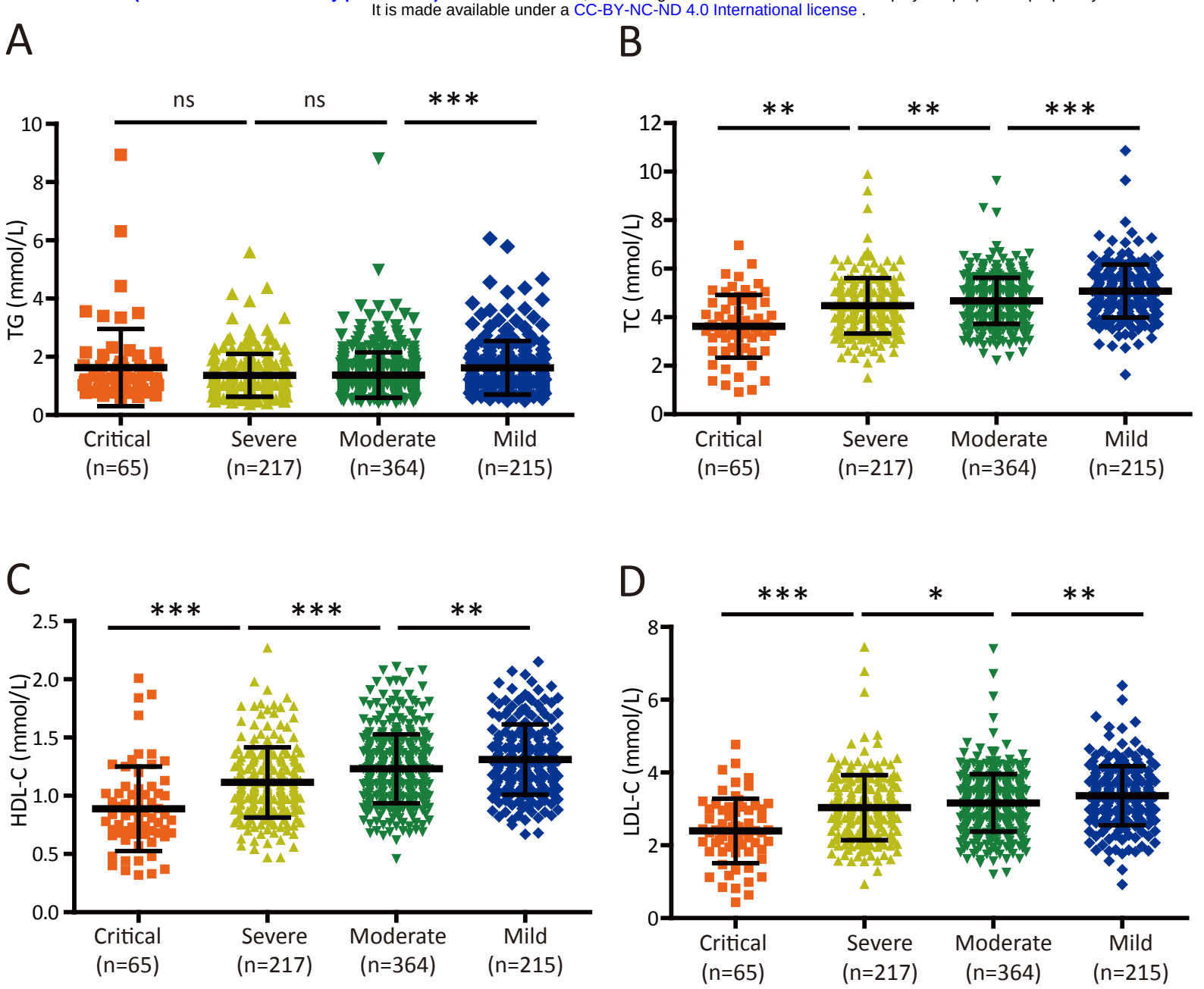

Figure 3

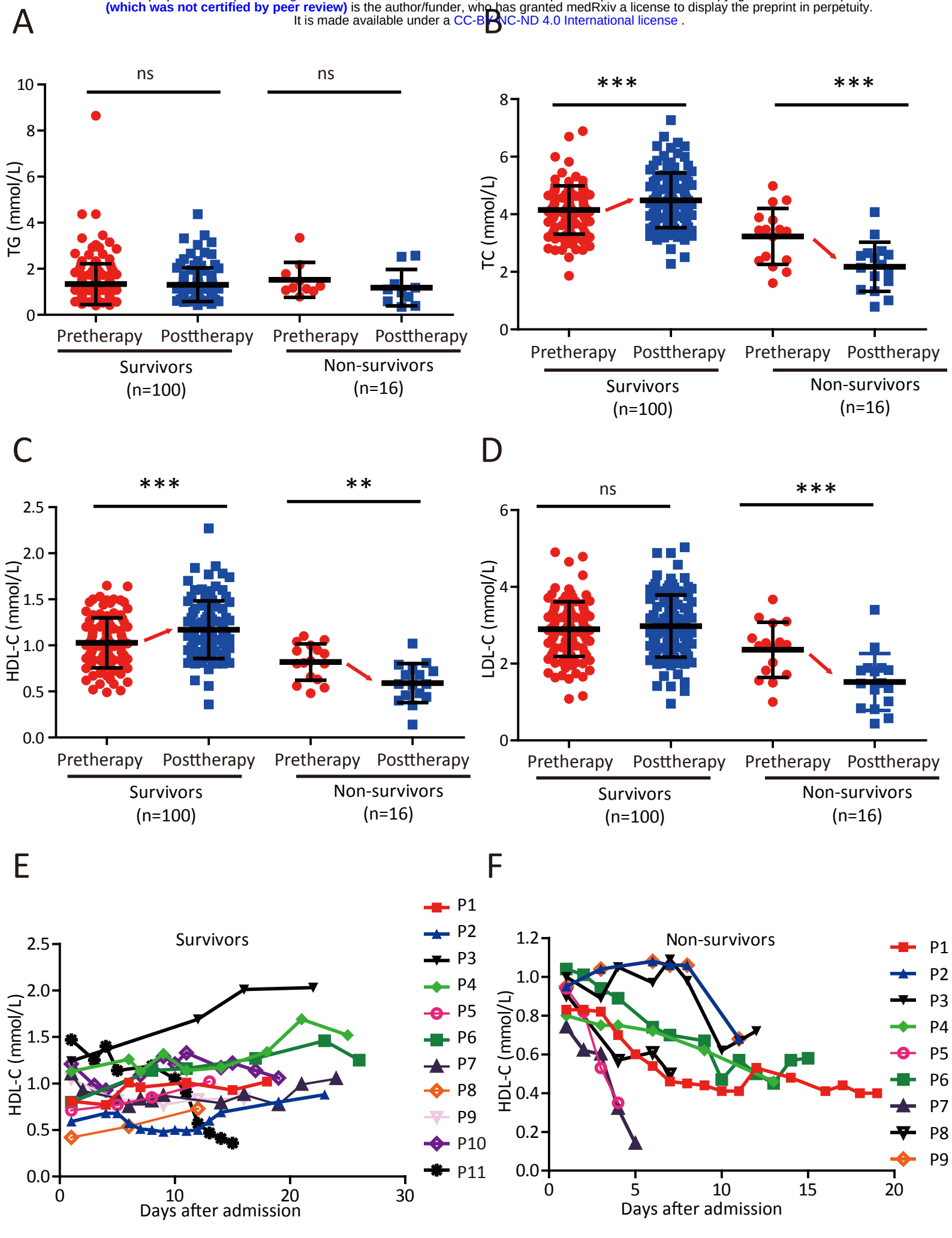

Figure 4

A

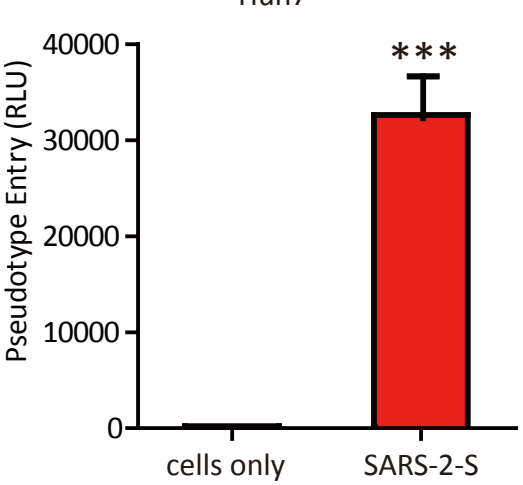

B

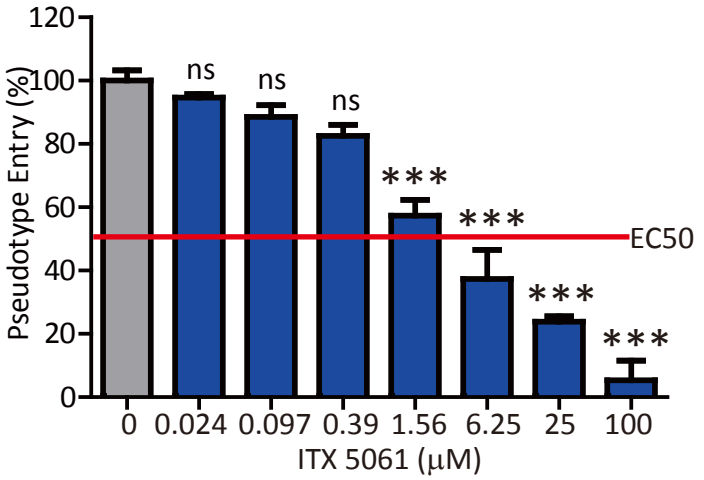

C

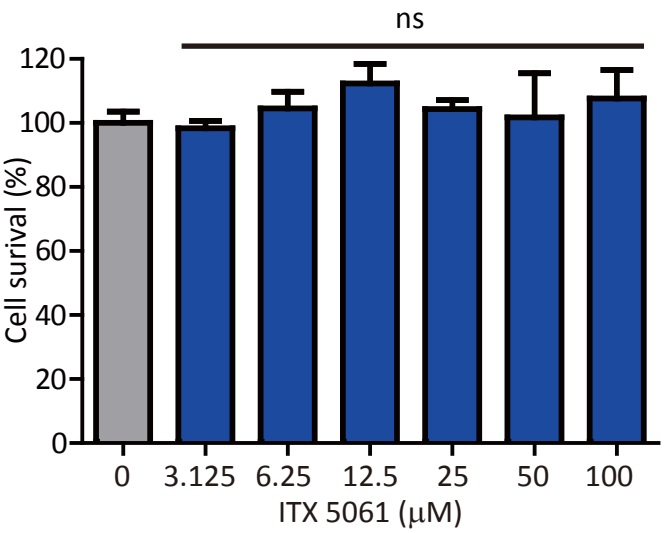

D

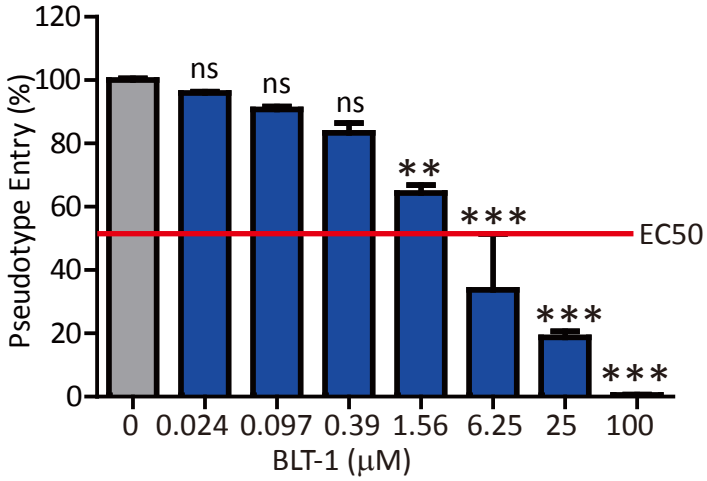

E

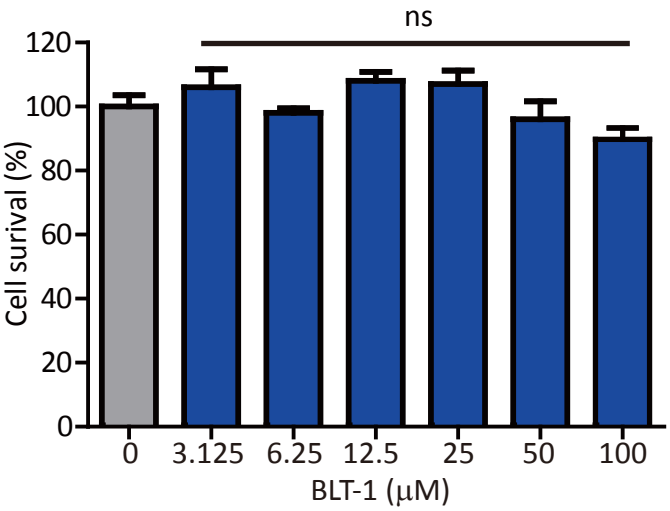

F

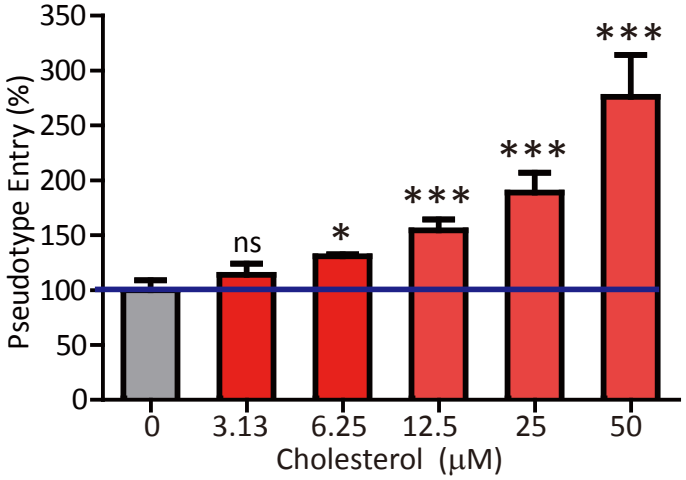

Figure 5

A

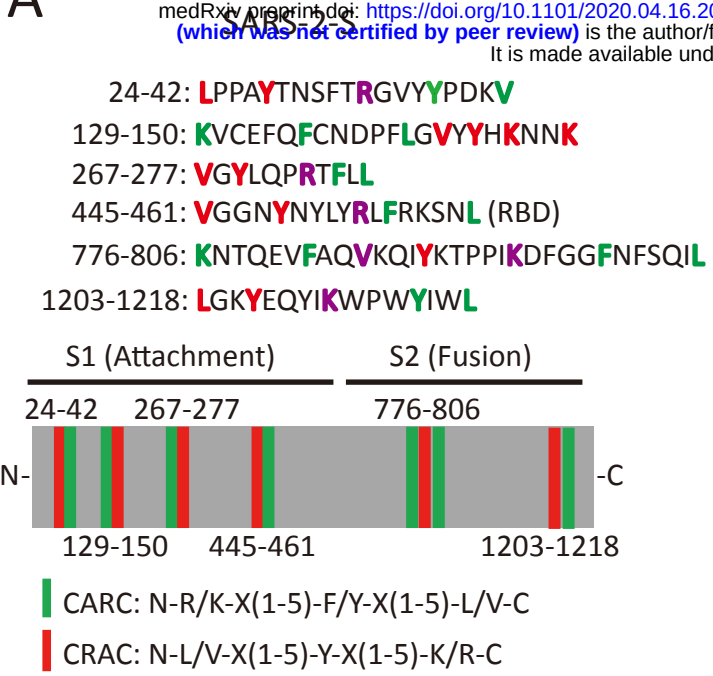

B

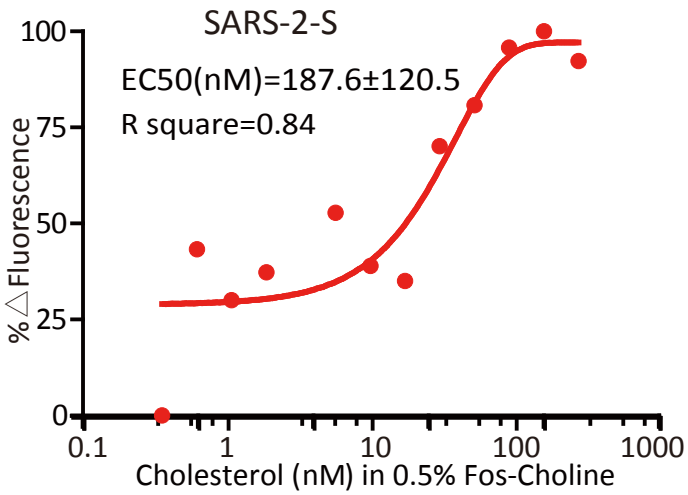

C

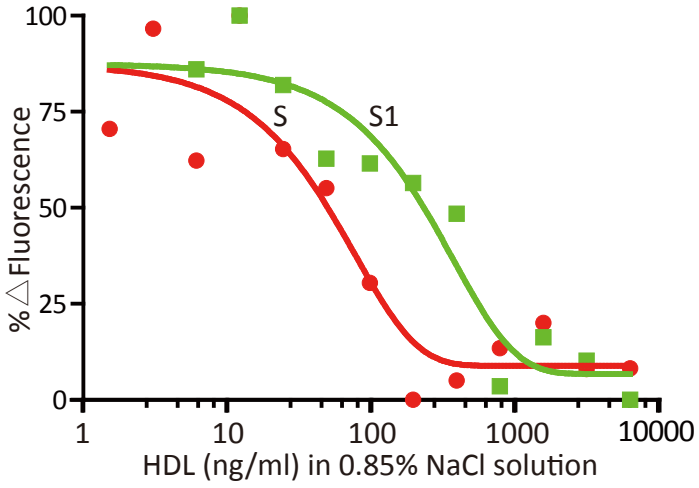

Protein	EC50 (ng/ml)	R square
S	55±25.4	0.88
S1	309±240.9	0.92

D